

SENSITIVITY OF COMPOSITE SCARF JOINTS TO MANUFACTURING DEVIATION AND DISBOND UNDER TENSILE LOAD

David J Larkin¹, Ioannis K Giannopoulos^{1*}, Efstathios E Theotokoglou²

¹*Centre of Excellence for Aeronautics, School of Aerospace, Transport and Manufacturing, Cranfield University, Cranfield, MK43 0AL, UK*

²*Department of Mechanics, Laboratory of Testing and Materials, School of Applied Mathematical and Physical Sciences, National Technical University of Athens, GR-157 73, Greece*

Abstract: Scarf joints are an effective method of bonding thick composite laminates for applications such as the repair of composite aircraft structures. However, concerns remain about their damage tolerance characteristics. Typically composite scarf repairs to aircraft structures require use of hand tools or rudimentary jigs. If the scarf is incorrectly prepared, this may cause a profile deviation to the joint, affecting the bond line stresses and in turn, reducing the residual strength of the joint or repair. The subject of this work examined the sensitivity of composite scarf joints to machining profile deviation and artificial disbond, when subject to static tensile load. Tensile test specimens were prepared with two different configurations of scarf for representing an undercut or imprecise scarf typical of a machining error. In addition, sensitivity of the scarf joints in the presence of an artificial disbond was also tested. Results indicated that for the specimens tested, the scarf is relatively insensitive to minor profile deviation, but highly sensitive to an artificial disbond. Experimental results were also compared with finite element analysis.

1. Introduction

From a joint efficiency perspective, carbon fiber composite laminates are best suited to adhesive bonding rather than mechanical fastening. Compared to bonded lap joints, scarf joints shown in figure 1, transfer load more efficiently through reduction of stress concentrations and load eccentricity.

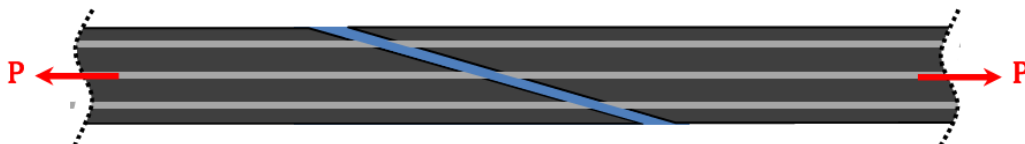


Figure 1: Scarf joint bonding between two composite laminated plates, under tensile loading

* Corresponding author

E-mail address: i.giannopoulos@cranfield.ac.uk

However, bonded joints are particularly sensitive to process and manufacturing flaws which degrade their strength and tolerance to service loading. This is even more pronounced with scarf joints due to their precision manufacturing requirements. Profile deviation from the ideal linear bond line caused by a machining error of the scarf end can lead to a change in the stress distribution, and may compromise residual strength of the joint. Research was conducted to study the effect of this bond line profile deviation and the partial disbond of the joint on the residual strength [1]. The various specimens manufactured are shown in figure 2.

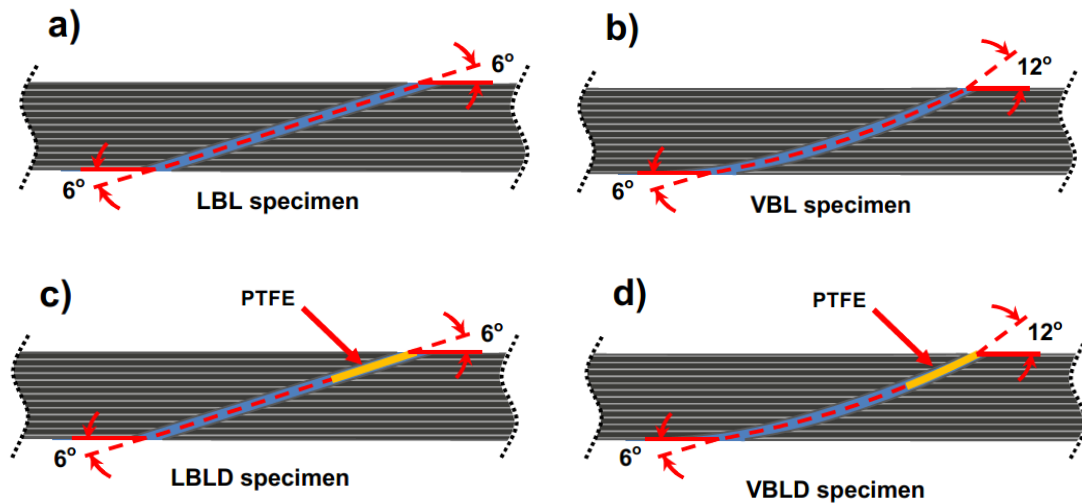


Figure 2: Different configurations of scarf, a) linear scarf angle bond line (LBL), b) variable scarf angles bond line (VBL), c) linear scarf angle bond line with artificial disbond (LBLD) and d) variable scarf angles bond line with artificial disbond (VBLD)

Ideal linear bond line (LBL) scarf joint type specimens were designed as shown in figure 2a) as well as variable scarf angle bond line (VBL) specimens for representing a possible machining error in the scarf angle prior to bonding. The VBL specimens were designed having a varying scarf angle θ along the length of the joint as shown in figure 2b). In addition, residual strength was examined both with and without an artificial disbond embedded in the bond line; specimens which are termed herein LBLD and VBLD and shown in figure 2c) and 2d) respectively. The artificial disbond represents an inclusion or adhesive failure along the edge of the joint and it was covering 25% of the total bond area, size dictated by the maximum in service load requirements as explained on the certification requirements section below.

2. Literature Review

Certification Requirements

The context of this research is to support the assessment and certification of composite bonded scarf joints and scarf repairs in the civil aircraft vehicle sector. In light of this, a brief discussion on the regulatory environment is important. This underpins the reason for why an understanding of such macro detail elements of joint design is required. Focusing on civilian requirements, EASA CS-25 and AMC-20-29 [2] define three methods to demonstrate compliance for certification of bonded primary structure:

(1) With the maximum possible disbond in place, the joint must still withstand limit load, (requirement to prove compliance to by analysis and/or test). It is difficult to quantify a maximum disbond size unless arresting features are used, effectively leading back to the use of mechanical fasteners.

(2) Proof testing to limit load has to be carried out on each production article. Whilst this might be acceptable for low production quantities and scales, this is cost prohibitive for transport category aircraft.

(3) Repeatable and reliable NDI needs to be established to ensure strength of every bonded joint. However, no existing Non Destructive Inspection (NDI) technique has been successful in reliably detecting the presence of an imperfect bond. Whilst NDI is effective at identifying inclusions and possibly voids, this will not always detect where an adhesive bond has not been made with the substrate.

Given the above problems, it is not possible to achieve the required level of quality assurance for certification of composite bonded joints for use in primary aircraft structure. In the knowledge that no perfect bond exists, where research can help to address this problem, is to develop a toolbox of techniques and capability to analyze the sensitivity of non-conformance and imperfection. The results of this could help to better define acceptable tolerances for manufacturing and repair quality control standards.

Previous Research

Previous research has focused on the optimization of scarf joints through analysis of the effect of different scarf joint design parameters. Foundational work by Erdogan & Ratwani [3] established numerical formulae for the analysis of scarf joints. This was followed by Hart-Smith [4] who further considered numerical analysis of composite scarf joints, dissimilar adherends and related step-lap joints. This early work showed the importance of maintaining a low scarf angle to resolve adhesive stress into the shear direction parallel to the bond line, rather than the peel direction which is transverse to the bond line.

More recent modelling by Gunnion & Herszberg [5] showed that the peak stresses in the adhesive decrease rapidly with reduction in scarf angle, being only limited by preventing breakage in the adherend tips. Indeed, an optimum scarf angle exists for a given adherend; according to Wang and Gunnion [6] this optimum angle occurs when the laminate-limiting strength equals the adhesive limiting strength. Thus, in the case of an optimally designed scarf joint but sub-optimally produced, there will be deviation on the residual strength of the joint. Moreover, pre-existing damage such as disbonds would also affect the residual strength of the joint. Such questions have been the subject of the research presented herein.

Research by Harman and Wang [7] investigated the optimization of scarf joints in order to make a uniform stress distribution across the joint for two dissimilar adherends. Harman and Wang achieved a near-constant stress distribution for isotropic adherends by varying the taper angle across the bond line, representing a geometrically ‘graded’ scarf joint.

Another factor to consider in the design of a composite scarf joint is the interfacing ply orientation. Research by Wang and Gunnion [6] and also Bendemra et al. [8] both concluded that peak adhesive shear stresses occur near the intersection of the zero degree plies with the adhesive. For orthotropic adherends Harman and Wang [7] proposed that reducing the taper

angle close to the zero degree plies can also help to reduce the stress concentration at these locations. Although it is not practical to implement this in a production or repair situation, it does identify that the location of deviations, disbonds and others, relative to the layup of the adherend will also affect the residual strength.

Previous research into damage tolerance aspects of scarf joint and repair design have sought to build on the knowledge base of understanding the effect of bond line flaws and how this translates to residual strength of the joint. Goh et al. [9] conducted research into the effect of an artificial bond line flaw of various sizes for a linear scarf joint. Goh found that residual static strength was highly sensitive to these flaws, reducing by 44% for a flaw size and specimen configuration similar to the one in this paper. The research herein will also consider bond line flaws, both with and without the presence of a profile deviation or ‘gradation’. Hayes-Griss et al [10] also conducted a similar investigation but this time considering two different linear 3° and 5° scarf joint specimens.

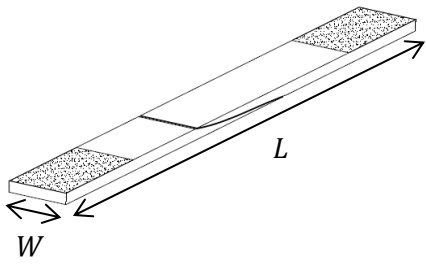
3. Experimental Methods

This investigation involved a substantial physical testing component, and was complimented by simulations using ABAQUS®. The subject of this paper is predominantly about the tensile testing activity. The configurations of scarf joints that are the subject of this paper are shown in figure 2.

Test Specimen Configuration

There is no pre-existing standard for the testing of composite scarf joints in the public domain. Therefore the specimen geometry chosen for this investigation consisted of an ASTM D3039 specimen modified with a scarf joint at the midpoint. The geometry is shown in table 1.

Table 1: Specimen Materials & Geometry

Design Basis:	ASTM D3039	Geometry:
Overall Length, L	250 mm	
Overall Width, W	25 mm	
Adherend thickness, $h_1 = h_2$	~4.72 mm	
Adhesive thickness, t_3	~0.25 mm	
Scarf angle, θ	6° -12°	
Overlap bond line length, ℓ	~42 mm	
Adherend UD Ply/Matrix	T800/M21	
Adhesive Material	FM94	
Adherend Layup	18 Ply, [+45/0/-45/90/0/+45/-45/0/90]s	

The laminate material consisted of 18 plies of M21/T800/35%/265GSM pre-preg, nominally 4.72mm thick when cured. The specimen halves were bonded along the scarf line with FM94 adhesive. A balanced, symmetric but non-quasi-isotropic layup was selected. The rationale for this selection was to provide an even distribution of zero degree plies throughout the layup, in order to somewhat stratify stress concentrations in the adhesive. All specimens were cut from a single laminate cured in accordance with manufacturer specifications.

Specimen Machining

The scarf angles were produced using Computer Aided Design and Manufacturing (CAD/CAM). Computer Numerical Controlled (CNC) machining shown in figure 3, utilized the input data from a 3D computer model of the specimens. The manufacturing deviation to the scarf angle was deliberately put into CAD software such that it would be replicated by CNC machining. Once the machining was complete, measurements were taken of the specimens using a digital caliper, in order to find the actual deviation (on top of the intended deviation) on the scarf angles. Of all the tensile test specimens, the lowest mismatch achieved was within 0.01 degrees, and the worst mismatch was 1.09 degrees. The average mismatch was 0.2 degrees for the linear scarf configuration and 0.8 degrees (measured at the midpoint) for the variable scarf angle bond line configuration.

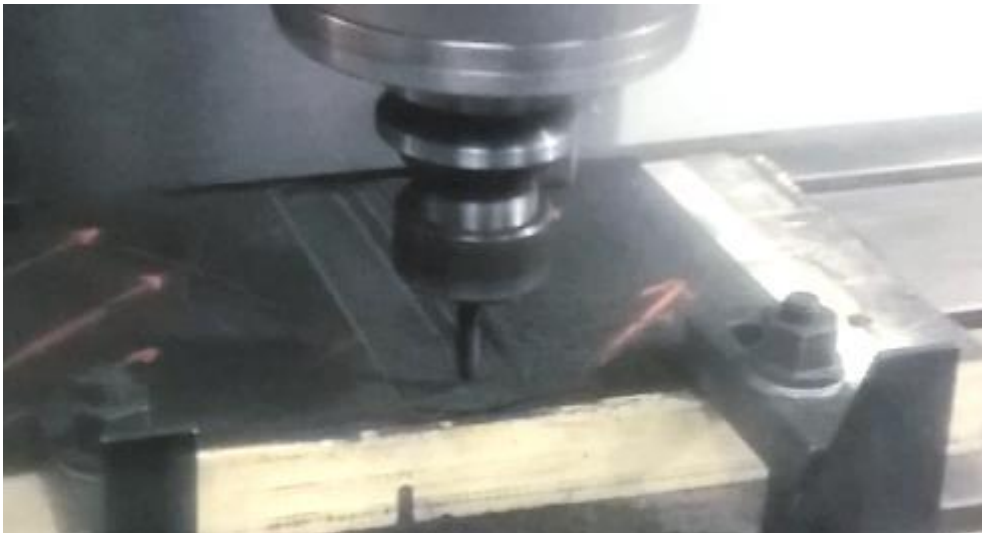


Figure 3: Machining of the composite panels before trimming

Specimen Bonding

Following machining, the next manufacturing process involved bonding the two scarf specimens using a custom-made precision bonding jig. The bonding jig was required to constrain the specimens in all dimensions to ensure that the bond line thickness was precisely controlled. This was achieved using a combination of adjustable end stops and rotating cams, to take-up any slight variations and allow for rapid assembly/disassembly. The jig configuration is shown in figure 4. In addition, the jig was required to apply the correct pressure to the specimens. This was achieved using custom-calibrated springs tightened to the correct extension to provide the required pressure to the cover plate. All specimens were subject to the same cure cycle consistent with the FM94 manufacturer requirements. Lastly, end tabs were also bonded using Redux 420. The use of end tabs was to ensure that failure occurred in the joint not the laminate.

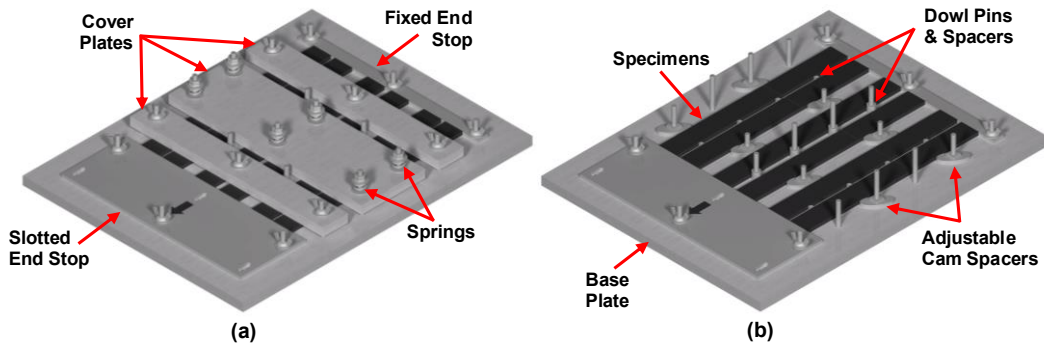


Figure 4: Multi-purpose bonding jig (a) with cover plates and (b) without cover plates

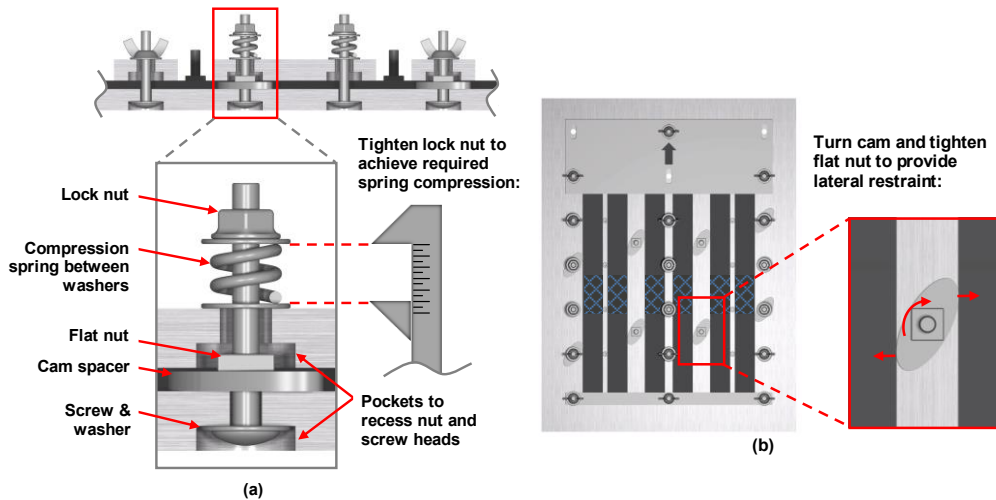
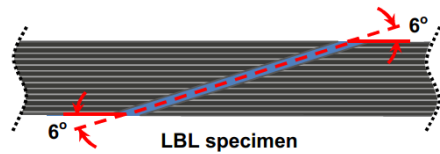


Figure 5: Cross section of the bonding jig showing (a) the adjustable spring mechanism and (b) the adjustable cam mechanism

Tensile Testing

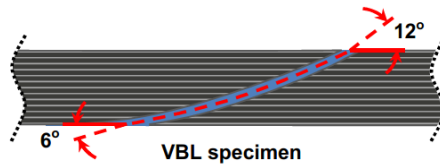
Tensile testing was carried out using a 100kN servo-electric test rig. The rig was connected to PC recording the load cell readout and cross head displacement. All specimens were tested to tensile failure and the load-extension relationship studied to examine the residual strength for the different configurations shown in table 2. Of these configurations half featured a partial disbond using Teflon PTFE tape. The test rig setup is shown in figure 6.

Table 2: Specimen design and number of articles tested



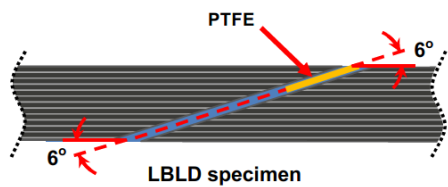
Linear Bond Line (LBL) specimens:

Three specimens with a linear scarf angle of 6°, without any artificial damage in the bond line



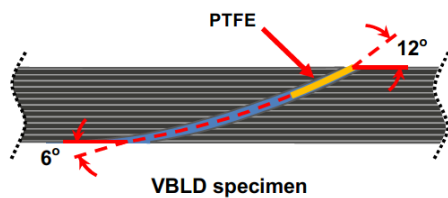
Variable Scarf Angle Bond Line (VBL) specimens:

Three specimens with a variable angle scarf angles of 6° and 12° at the edges, without any artificial damage in the bond line



Linear bond line specimens with damage (LBLD):

Three specimens with a linear scarf angle of 6°, with artificial delamination at one edge



Variable scarf angle bond line specimens with damage (VBLD):

Three specimens with a variable angle scarf angles of 6° and 12° at the bond line edges, with artificial delamination implemented on the 12° exit edge

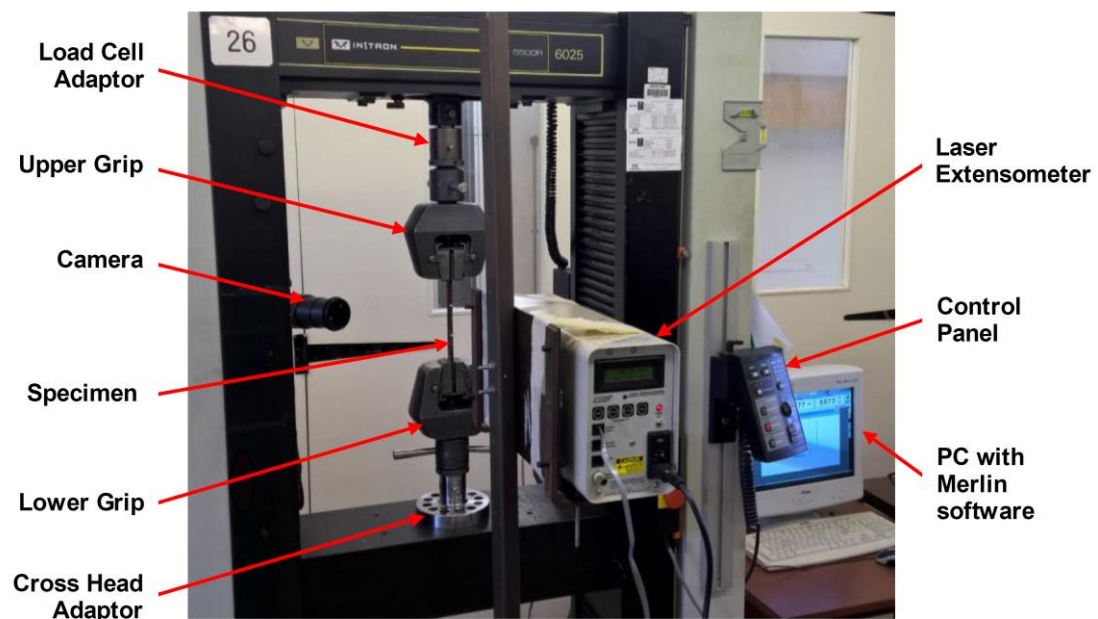


Figure 6: Tensile test rig and instrumentation

Micrographic Inspection

Following completion of the tensile testing, the samples were inspected under an optical microscope. The purpose of this activity was to identify the failure mechanism and see if this was influenced by the different scarf configurations. However, results predominantly showed a mixed mode of failure across all bond surfaces picture consistent across all the samples tested. However, specimens with linear scarf joints showed a more consistent ‘zebra-striped’ mixed adhesive-cohesive failure surface in contrast to the variable angle scarfs were adhesive failure was more pronounced. An example of a single post-failed specimen side is shown in figure 7.

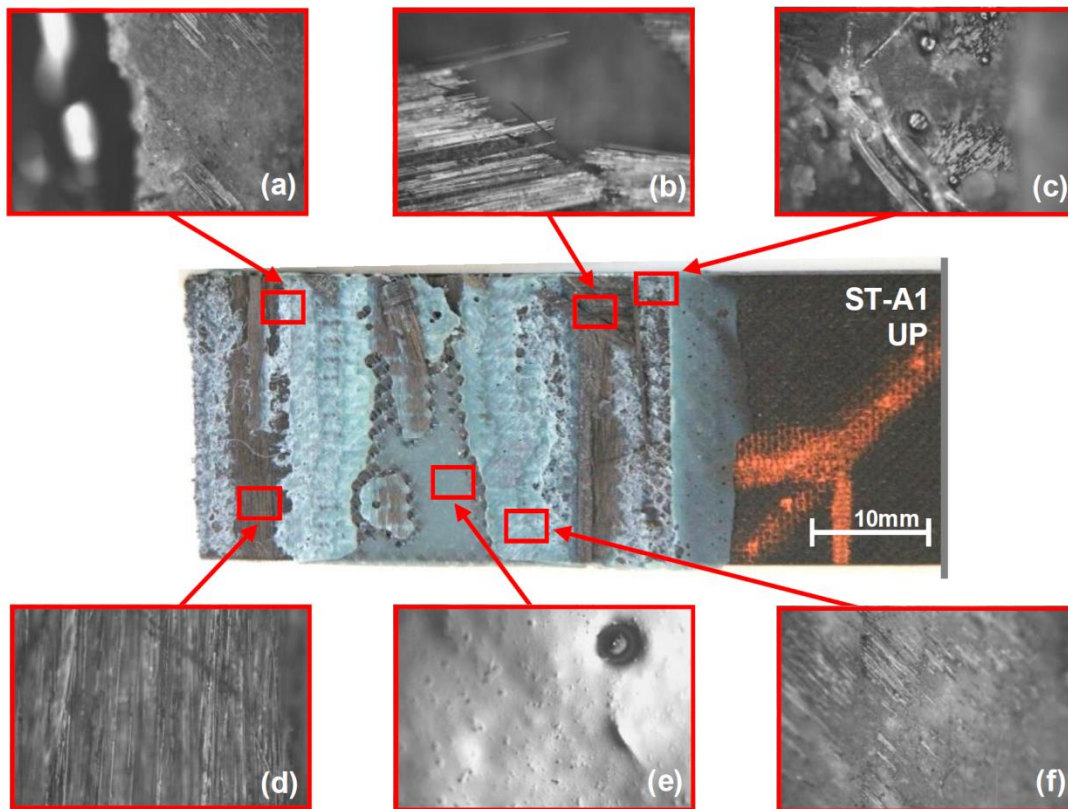


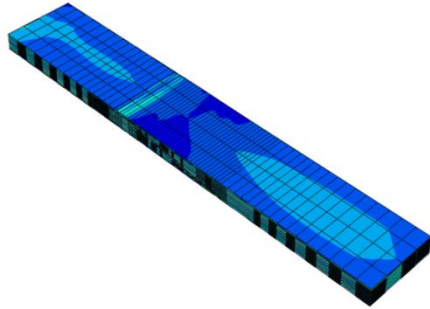
Figure 7: Micrographic images of one tensile specimen. Insets at 10x magnification showing adhesive failure at locations (a) and (f), cohesive failure at (c), fiber breakage (b) and (d), and voiding/kissing bond (e)

Finite Element Analysis

Finite Element Analysis (FEA) was carried out using ABAQUS® [11]. The purpose of this activity was to explore further combinations of variations to the configuration and also to benchmark some of the physical test results. The model was a 3D continuum shell with a traction-separation relationship applied to the bond line. This of course was a simplified model, as through-thickness adhesive effects were not modelled i.e. it is assumed that the bond is very thin compared to the laminate. For a scarf joint, the thickness of the tips approaches the thickness of the adhesive. Nonetheless, the FEA modelling demonstrated failure behavior consistent with the physical model. Details of the model are shown in table 3.

Notably, the FEA geometry is 100mm shorter than the physical test specimen. This is because the area under the tab ends did not need to be modelled, and these were addressed through application of suitable boundary conditions to each end of the specimen. The parameters varied for the FEA model include the scarf angle and the size of the disbond. Indicative boundary conditions are shown in figure 8.

Table 3: Finite Element Model Details and Geometry

Design Basis:	N/A	Geometry:
Number of Elements	~7450	
Adherend Element Formulation	Continuum Shell	
Adherend Element Type	SC8R Hex	
Adhesive modelling	Traction separation	
Overall Length, L	150 mm	
Overall Width, W	25 mm	
Adherend thickness, $t_1 = t_2$	4.72 mm	
Adhesive thickness, t_3	0.25 mm	
Scarf angle, θ	6° -12°	
Overlap bond line length, ℓ	~42 mm	
Adherend Layup	18 Ply, [+45/0/-45/90/0/+45/-45/0/90]s	
Material Properties	T800/M21 & FM94 where available	

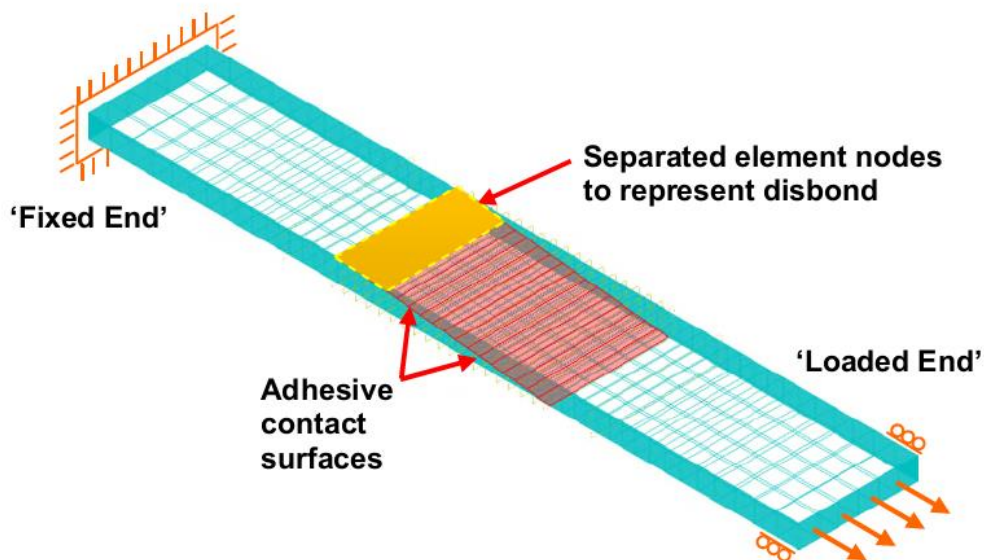


Figure 8: Indicative boundary conditions and contact surfaces for FEA model

4. Results & Discussion

Physical Testing

Results of the tensile tests are depicted in figure 9. The test results showed that the variable scarf angle specimens, failed on average 14% lower load than the linear scarf. When a PTFE insert is introduced, representing a 25% disbond; a dramatic 45% reduction in failure load was seen compared to the non-artificially damaged joints. The reduction in load in the presence of a disbond for the linear specimens, agreed well with the 44% reduction seen by Goh et al. [9], for a similar flaw size. There were a total of 12 tensile tests carried out; three of each specimen configuration. Comparing both linear and variable scarf profiles in the presence of a disbond, the failure loads were relatively invariant.

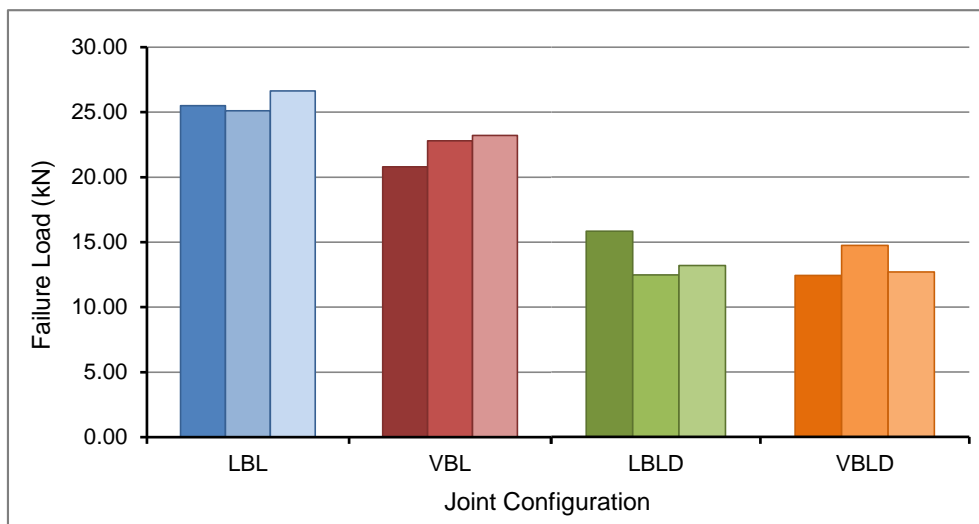


Figure 9: Tensile test results for different specimen configuration groups

Failure behaviour of the VBL scarf was also typified by higher apparent failure strains, but this is difficult to attribute. It was noted that all scarfs were cut from the same laminate, machined and surface prepared in the same way, and bonded and cured under the same conditions. Interrogating the quality control data (measurements, thermography scans, etc.) also did not explain this diverse failure spread. At least for these configurations it was shown that the VBL scarf did not result in a dramatic reduction in failure load compared to LBL. The far more severe effect is that of a partial disbond (LBLD/VBLD). This suggested that the sensitivity of scarf joints to bond line variation is far less pronounced than inclusions, bonding flaws or progressive delamination.

Finite Element Modeling

Behaviour of the FEA model agreed well with the physical testing but with a higher failure load by about 20% compared to the physical testing. Some explanations for this include the adhesive and laminate properties used for the simulation which were acquired from published manufacturer material data and/or derived from previous testing surveys; from imperfect surface preparation on the physical test specimen and environmental factors which may have reduced the performance compared to the 'perfect and ideal' behavior. For linear scarf joints, the bonds were found to fail at the outer edges first and progress inwards as shown in figure 10. For the partially disbanded FEA models, the reduction in failure load was comparable to the physical test specimens.

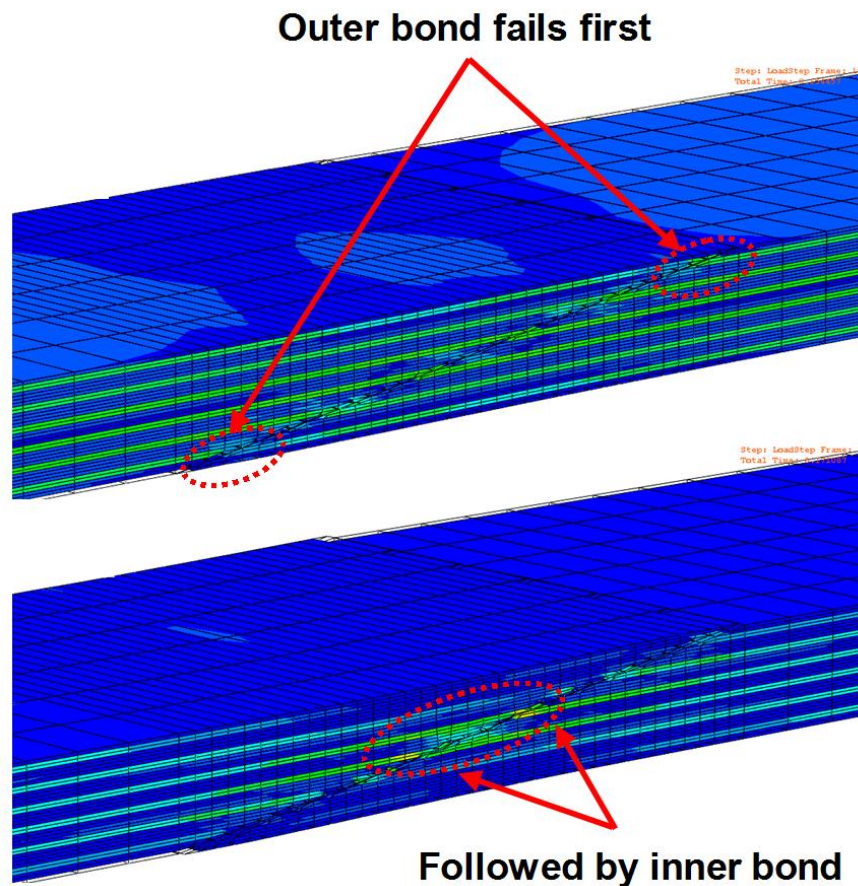


Figure 10: Finite element model of a linear, pristine scarf, showing failure sequence; peak stresses are coincident with the zero degree plies.

5. Conclusions

These results indicate that scarf joints are particularly sensitive to disbonds, but relatively insensitive to profile deviation at the angles tested. It is theorized that sensitivity to a disbond in the presence of a profile deviation is highly dependent on the location of the disbond, and this is an avenue of further testing. Further testing should be carried out to explore the trend seen of higher failure strain in the presence of a variable scarf angle. It is plausible that a joint could also be optimized to incorporate a gradation, potentially to exploit this phenomenon of higher failure strain, albeit with a slight reduction in static strength. However, such concepts must be balanced against the requirement to manufacture the joint in a repeatable and quality-assured manner, and to account for all loading scenarios and real-world damage characteristics.

References

- [1] Larkin D.J. (2016). *Damage Tolerance of a Graded Scarf Joint for Composite Aircraft Structures*, MSc Thesis, Cranfield University, Bedfordshire.
- [2] European Aviation Safety Agency, (2010). *EASA AMC 20-29 – Composite Structure. Acceptable Means of Compliance*. European Aviation Safety Agency, Cologne.
- [3] Erdogan F., Ratwani M. (1971). *Stress Distribution in Bonded Joints*. Journal of Composite Materials. Vol 5, p. 378–393.
- [4] Hart-Smith L.J. (1973). *NASA-CR-112237 - Adhesive-Bonded Scarf and Stepped-Lap Joints*. National Aeronautics & Space Administration, Hampton.
- [5] Gunnion A.J., Herszberg I. (2006). *Parametric Study of Scarf Joints in Composite Structures*. Composite Structures. Vol 75, p. 364–376.
- [6] Wang C.H., Gunnion A.J. (2008). *On the design methodology of scarf repairs to composite laminates*. Composites Science and Technology. Vol 68, p. 35–46.
- [7] Harman A.B., Wang C.H. (2006). *Improved design methods for scarf repairs to highly strained composite aircraft structure*. Composite Structures. Vol 75, p. 132–144.
- [8] Bendemra H., Compston P., Crothers P.J. (2015). *Optimisation study of tapered scarf and stepped-lap joints in composite repair patches*. Composite Structures. Vol 130, p. 1–8.
- [9] Goh J.Y., Georgiadis S., Orifici A.C., Wang C.H. (2013). *Effects of bondline flaws on the damage tolerance of composite scarf joints*. Composites Part A: Applied Science and Manufacturing. Vol 55, p. 110–119.
- [10] Hayes-Griss J.M., Gunnion A.J., Afaghi Khatibi A. (2016). *Damage tolerance investigation of high-performance scarf joints with bondline flaws under various environmental, geometrical and support conditions*. Composites Part A: Applied Science and Manufacturing. Vol 84, p. 246–255.
- [11] Abaqus-Inc. Abaqus 6.14 - Analysis user's guide volume II: Analysis. Providence, RI: Dassault Systèmes Simulia Corp.; 2014.

Sensitivity of composite scarf joints to manufacturing deviation and disbond under tensile load

Larkin, David J.

2017-06-30

Larkin D, Giannopoulos I & Theotokoglou E (2017) Sensitivity of composite scarf joints to manufacturing deviation and disbond under tensile load. In: 14th International Conference on Fracture (ICF14), Rhodes, 18-23 June 2017.

<https://dspace.lib.cranfield.ac.uk/handle/1826/12136>

Downloaded from CERES Research Repository, Cranfield University